1st International Conference on Sensing Technology
November 21-23, 2005 Palmerston North, New Zealand

Accurate Model of Saturated AMR Wheatstone Bridge Sensor Against a 48 Pole Pair Ring-Magnet.

Michael J. Haji-Sheikh
Electrical Engineering Department
Northern Illinois University
De Kalb, Illinois
Mhsheikh@ceet.niu.edu

Abstract

Presented is a method to model a magnetoresistive Wheatstone bridge using a new magnetoresistive model for resistor elements in saturation. This new model accurately predicts the behavior of individual magnetoresistors and follows the form $\Delta R/R_0=A+B((1+C*\cos(2\theta)^2+C*\sin(2\theta)^2)$. To demonstrate the use of this model, a 17.5nm thick permalloy sensor bridge was used to sense a forty-eight pole pair ring magnet. The results show a good correlation between the model and an actual device under test.

KEYWORDS: PERMALLORS, AMR, SATURATION, RING MAGNETS

1 INTRODUCTION AND THEORY

The magnetoresistive sensor element has become an industrial and commercial mainstay in the world of sensors. Since the mid 1960's, when the development of high quality vacuum deposition systems for the fledgling integrated circuit business made it possible to deposit high quality thin films, people have been developing thin film magnetoresistive sensors from anisotropic magnetoresistive (AMR) films. Memory devices were conceived to take advantage of the planer Hall-effect [1] and the beginnings of the first models were also conceived at this time. The applications for anisotropic magnetoresistors range from computer hard drives, magnetometers to engine crank sensing. A common use of magnetoresistive sensors is the detection of the angle from which any given external field is coming. This type of angle sensor is common in automotive applications. It is important, for most of these applications, to be able to accurately predict this behavior. The development of sensors lead to the development of mathematical models which represent the behavior in such a way as to reduce the design cycle time. Most models can date back to the research work done by the people at IBM's Watson Research Center [2,3]. The classic model as represented by Eijkal and Fluitman [4] does not separate the isotropic properties of the resistivity from the anisotropic components due to magnetization. Figure 1 shows a schematic representation of the proposed resistor model.

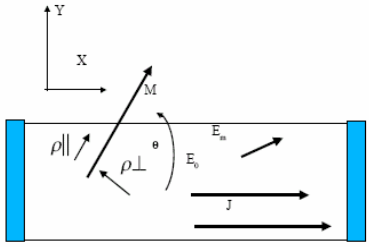

Figure 1. Schematic of a anisotropic magnetoresistor. The electric field due in this model is represented by an isotropic component and a magnetic component and the current density points in the x-direction.

A magnetoresistive model is normally represented by the following conditions

$$\Delta\rho=(\rho\|-\rho\perp)/2 \qquad (1)$$

$$\frac{\Delta\rho}{\rho}=\frac{\rho\|-\rho\perp}{\rho\|+\rho\perp} \qquad (2)$$

$$\rho=(\rho\|+\rho\perp)/2 \qquad (3)$$

whereas these conditions with a minor modification can be rewritten to account for the isotropic sources of resistance. The rewritten form of these conditions is as follows,

$$\rho\|=\rho'\|+\rho_0 \qquad (4)$$

$$\rho\perp=\rho'\perp+\rho_0 \qquad (5)$$

$$\Delta\rho' = \frac{\rho'\| - \rho\perp}{2} = \Delta\rho \quad (6).$$

A two-dimensional tensor best represents the thin film magnetoresistors. The tensor for a the two-dimensional case is

$$\mathrm{P} = \begin{bmatrix} \rho\| & 0 \\ 0 & \rho\perp \end{bmatrix} \quad (7),$$

with ρ|| and ρ⊥ tied to the direction of the magnetization. A detailed solution, which outlines the modified approach, is shown in Haji-Sheikh [5]. To solve for the resistance of any individual resistor, the tensor must be transformed to the direction of the current density. The final transformation creates the following transformed tensor

$$\mathrm{P'}_{total} = \mathrm{P'}_0 + \mathrm{P'}_{magnetic} \quad (8)$$

where

$$\mathrm{P'}_{tot} = \begin{bmatrix} \rho_0 & 0 \\ 0 & \rho_0 \end{bmatrix} + \begin{bmatrix} \rho' + \Delta\rho'\cos(2\theta) & \Delta\rho'\sin(2\theta) \\ \Delta\rho'\sin(2\theta) & \rho' - \Delta\rho'\cos(2\theta) \end{bmatrix} \quad (9).$$

This solution can be used to determine the electric field for a x-direction current by

$$\begin{bmatrix} E'_x \\ E'_y \end{bmatrix} = \begin{bmatrix} \rho_0 & 0 \\ 0 & \rho_0 \end{bmatrix} \begin{bmatrix} J \\ 0 \end{bmatrix} + \begin{bmatrix} \rho' + \Delta\rho'\cos(2\theta) & \Delta\rho'\sin(2\theta) \\ \Delta\rho'\sin(2\theta) & \rho' - \Delta\rho'\cos(2\theta) \end{bmatrix} \begin{bmatrix} J \\ 0 \end{bmatrix} \quad (10).$$

The effective resistivity of a single element under test will then be represented by

$$\rho_{eff} = \rho_0 + \rho' \left(\left(1 + \frac{\Delta\rho'}{\rho}\cos(2\theta) \right)^2 + \left(\frac{\Delta\rho'}{\rho}\sin(2\theta) \right)^2 \right)^{\frac{1}{2}} \quad (11).$$

The following voltage equation can then be used to fit actual resistors

$$V_{total} = I_s R_0 (A + B((1 + C\cos(2\theta))^2 + (C\sin(2\theta))^2)^{\frac{1}{2}}) \quad (12).$$

The coefficients A, B and C can be obtained empirically from the measurements. Figure 2 is such a measurement and demonstrates how well the equation [12] fits the actual data. Table I shows coefficients obtained by the typical measurements shown in Figure 2.

Table I. Coefficients for normalized resistance.

	A	B	C
5nm Film	0.9472	0.0192	0.3545
20nm Film	0.9719	0.0176	0.6540
37.5nm Film	0.9700	0.0163	0.8540

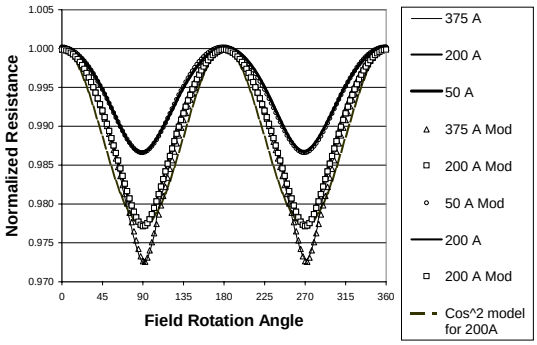

Figure 2. Magnetoresistance of three different saturated magnetoresistors versus the externally applied field direction. This graph shows the model fit for the 5nm, 20nm, 37.5nm and the 20nm $\cos^2\theta$ fit. It appears that the $\cos^2\theta$ model has the periodicity but not the shape of the data.

The resistance portion of the equation (12) then can be used to build a Wheatstone bridge consisting of zero-degree elements and ninety-degree oriented elements. A typical bridge of the preceding type is shown in Figure 3.

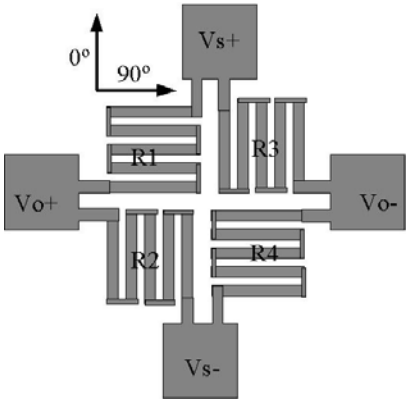

Figure 3. Schematic of a typical 0°-90° magnetoresistor used in this experiment. This sensor is a classic Wheatstone bridge.

The bridge is a voltage divider and can be solved by the following relationship

$$\Delta V = V_0 \frac{R2}{R2 + R1} - V_0 \frac{R4}{R3 + R4} \quad (13)$$

and

$$R1 + R2 = R3 + R4 \quad (14)$$

so

$$\Delta V = V_0 \frac{R2 - R4}{R2 + R1} \quad (15).$$

Each of the individual resistor elements has the same nominal resistance so that the resistors can be represented by

$$R1 = R_0(A + B((1 + C\cos(2\theta))^2 + (C\sin(2\theta))^2)^{\frac{1}{2}}) \quad (16)$$

$$R2 = R_0(A + B((1 + C\cos(2(\theta + 90^0)))^2 + (C\sin(2(\theta + 90^0)))^2)^{\frac{1}{2}}) \quad (17)$$

$$R2 = R3 \quad (18)$$

$$R1 = R4 \quad (19)$$

Replacing the individual resistors with the above equations creates a sensor bridge whose output is dependent on the angle of the external field.

2 EXPERIMENTAL PROCEEDURE AND RESULTS

Angle sensors were fabricated using a standard VLSI processing equipment and surface micro machining [6]. The starting material was n-type (100) silicon which had 500 nm of thermally SiO_2 grown on the top surface. A multilayer film of TaN/$Ni_{81}Fe_{19}$/TaN was deposited using a radio frequency magnetron deposition system. The deposition system used to produce this sensor film was a Materials Research Corporation 603-4 with a custom cathode specifically designed for the deposition of permalloy. The targeted thickness of the $Ni_{81}Fe_{19}$ permalloy film used for this experiment was 17.5 nm. This thickness was chosen for its sensitivity and resistivity to achieve a specific design goal not pertinent to this paper. The resistors were patterned using a positive photoresist and the pattern was etched into the film using a VEECO ion-mill.

The resistor elements were connected together using plasma deposited TiW/Al interconnect metal and wet etched. Figure 3 is a cross-section of a magnetoresistor produced with the above process. The sensors were then passivated with PECVD silicon nitride then post annealed to minimize the total resistance.

Testing to correlate the response of a single resistor element was performed using a probe station modified with x-y air core Helmholtz coils. Each Helmholtz coil was calibrated with a Gauss probe traceable to NIST. Initial testing was performed to determine what was the field required to saturated a test resistor. Due to this testing, a field of 30 Gauss was chosen. This field was then rotated through 360° degrees by 0.1° steps to help determine the modeling coeifficients.

Sensor die were constructed using the same processes used to build the test die. Individual sensor die were singulated and mounted in a commercially available molded plastic packaging. A schematic of the test setup for the sensor bridge to sense a ring magnet is shown in Figure 5. Figure 6 demonstrates how a ring magnet is arranged with alternating north south poles. The pole transitions on a 48 pole pair ring magnet occur every 3.75° of rotation. This means that the magnetic field rotates 360° for every 7° of ring magnet rotation.

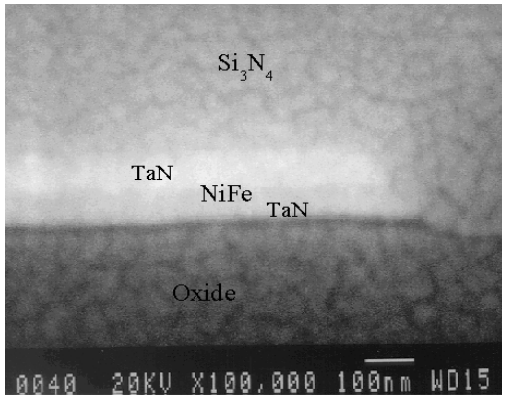

Figure 4. Cross-section of an AMR (anisotropic magnetoresistor) sensor element. Magnification 10000X.

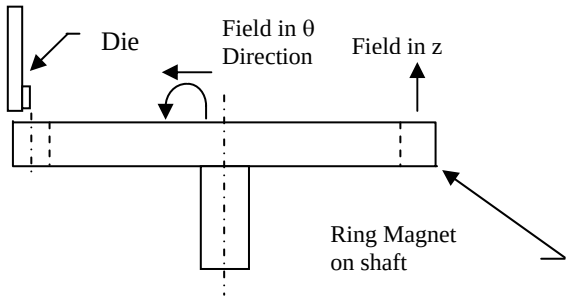

Figure 5. Ring Magnet test structure. The ring magnet consists of 48 pole pairs. The magnetic field in the area of the die (sensor bridge) rotates 360° for every North-South-North transition.

Figure 7 shows the results of one of these individual die against a 48 pole pair ring-magnet mounted on a stepping motor shaft. This graph shows both the results of the model and data (for two different gap spacings) versus the angular rotation of the spindle. The gap spacing is the distance of the sensor from the surface of the ring magnet and not the distance between the package molding and the magnet. The gap spacing used in this comparison produced saturated or nearly saturated sensor elements which in turn allow for the model not to have to deal with the effect of magnetization reversal [7]. The bridge bias is 2.4 V which produces an output of the bridge which is ±20mV. This corresponds to a sensitivity of 21mV per degree of spindle rotation.

Figure 8 is a plot of output voltage versus the spindle rotational angle for north-south transition. This plot shows both the quality of fit between the

model and the data and the issue of magnetization reversal as the field rotates out of one sensor quadrant to the next sensor quadrant. The 1.5mm gap spacing shows very good correlation between the model and actual data.

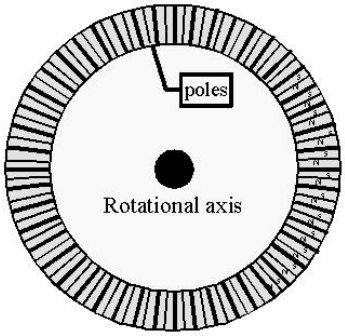

Figure 6. Schematic top view of a 48 pole pair ring magnet. This schematic shows how a ring magnet alternates the magnetic poles. Narrow lines represent north-south transitions.

There is some error at the positive voltage output. The mismatch means that the "zero" crossing regions have the highest accuracy to spindle angle and the maximum and minimum values have the least accuracy. There will be some additional errors due to ring magnet manufacturing tolerences. The total error of the system, at zero crossing (ring magnet and sensor), appears to be less than 0.2° of spindle rotation. The bridge model clearly demonstrates the same basic response as the actual resistor. This is not only apparent at the zero crossing but also with the basic curve shape. This shape of the wave is roughly triangular. Due to the 2θ behavior of the sensor elements, the sensor will have 2 full cycles for every pole pair. The 2.0mm gap spacing puts the sensor slightly out of saturation as compared with the 1.5mm gap spacing. The comparison of the $\cos^2 \theta$ model shows that the $\cos^2 \theta$ over-predicts sensitivity.

3 CONCLUSION.B

It is possible with the modeling approach outlined to reasonably simulate the response of a magnetoresistive Wheatstone bridge under saturation conditions. Both the zero crossing and the waveform of the model replicate the actual device under saturation. Under close inspection, it appears that there is a small error at the maximum and minimum points due to minor magnetization reversal issues and a small error at the "zero" crossing points. This model accurately represents the ideal ring-magnet and sensor pair while the ring magnet does have some error due to manufacturing tolerances.

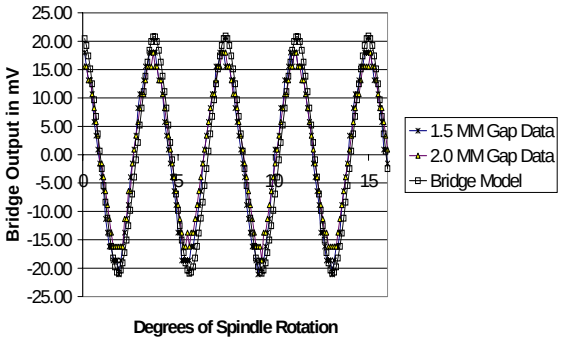

Figure 7. Comparison of experimental magnetoresistor bridge and the bridge model versus the angle of rotation for a ring magnet on a spindle. The model assumes that the field saturates the magnetoresistor and the external field rotates 360° every 7.5° of spindle rotation.

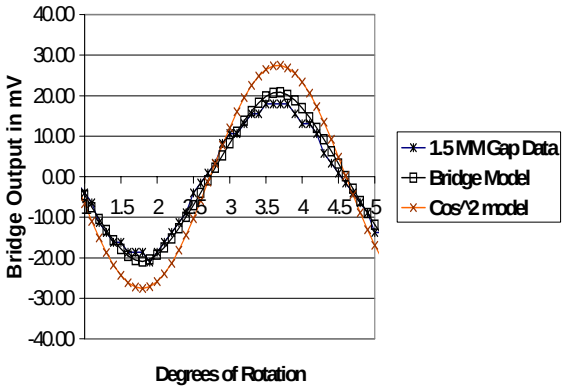

Figure 8. Comparison of experimental magnetoresistor bridge and the bridge model versus the angle of rotation for a ring magnet on a spindle. The model assumes that the field saturates the magnetoresistor and the external field rotates 360° every 7.5° of spindle rotation. The $\cos^2 \theta$ model over predicts the sensitivity of the 200 angstrom sensor.

4 ACKNOWLEGEMENTS

Special thanks to Ernie Brose (retired), Perry Holman and Rich Kirkpatrick of Honeywell International.

5 REFERENCES

[1] C.P. Batterel and M. Galinier, "Optimization of the planar hall effect in ferromagnetic thin films for device design ", IEEE Trans. Magn. MAG-5, 18 (1969)

[2] T. R. McGuire and R. I. Potter," Anisotropic magnetoresistance in ferromagnetic 3d alloys", IEEE Trans. Magn. MAG-11, No. 4,1018 (1975)

[3] D. A. Thompson, L. T. Romankiew, and A. F. Mayadas," Thin film magnetoresistors. in memory, storage, and related application", IEEE Trans. Magn. MAG-11, No 4, 1039 (1975)

[4] K. J. M Eijkel and J. H. J. Fluitman, "Optimization of the response of

magnetoresistive elements", IEEE Trans. Magn. 26, No. 1, 311 (1990)

[5] M. J. Haji-Sheikh, G. Morales, B. Altuncevahir, and A. Koymen, "Anisotropic Magnetoresistive Model for Saturated Sensor Elements.", IEEE Sensors Journal, accepted Sept. 2004.

[6] M. J. Haji-Sheikh, "TaN/NiFe/TaN Anisotropic magnetic sensor element", U. S. Patent No. 5667879

[7] P. A. Holman, Ph.D. Dissertation, "Design Model of Longitudinal Magnetoresistance of PermalloyPrior to Magnetization Reversal," University of Texas at Dallas, 2003